

Expression and prognostic analyses of SCAMPs in pancreatic adenocarcinoma

Feiyu Mao^{1,*}, Heng Duan^{2,*}, Aly Allamyradov¹, Zechang Xin², Yan Du², Xiaodong Wang³, Peng Xu³, Zhennan Li³, Jianjun Qian³, Jie Yao^{1,3}

¹Clinical Medical College of Yangzhou University, Yangzhou 225001, Jiangsu Province, China

²The First Affiliated Hospital of Dalian Medical University, Dalian 116044, Liaoning Province, China

³Department of Hepatobiliary and Pancreatic Surgery, Northern Jiangsu People's Hospital, Guangling Qu, Yangzhou 225001, Jiangsu Province, China

*Co-first authors

Correspondence to: Jie Yao; email: docyao@hotmail.com, <https://orcid.org/0000-0001-5447-893X>

Keywords: SCAMPs, differential expression, prognostic biomarkers, pancreatic adenocarcinoma

Received: July 1, 2020

Accepted: November 23, 2020

Published: January 20, 2021

Copyright: © 2021 Mao et al. This is an open access article distributed under the terms of the [Creative Commons Attribution License](https://creativecommons.org/licenses/by/3.0/) (CC BY 3.0), which permits unrestricted use, distribution, and reproduction in any medium, provided the original author and source are credited.

ABSTRACT

Due to the difficulties in early diagnosis of pancreatic adenocarcinoma (PAAD), many patients fail to receive optimal therapeutic regimens. The Secretory-Carrier-Membrane-Proteins (SCAMPs) are known to be dysregulated in a range of human diseases due to their characterized roles in mammalian cell exocytosis inferred from their functions as integral membrane proteins. However, the expression and prognostic value of SCAMPs in PAAD is poorly characterized. We compared cancer vs. healthy tissue and found that the expression of SCAMPs1-4 was upregulated in PAAD compared to normal tissue. In contrast, SCAMP5 expression was downregulated in PAAD. Moreover, the expression of SCAMPs1-4 was enhanced in PAAD cell lines according to Cancer Cell Line public database. Furthermore, the HPA, GEPIA databases and immunohistochemical analysis from 238 patients suggested that the loss of SCAMP1 led to improved overall survival (OS), whilst lower SCAMP5 levels led to a poorer OS. The univariate and multivariate analysis showed that SCAMP1 and SCAMP5 expression were independent prognostic factors of PAAD. In addition, the cBioPortal for Cancer Genomics, LinkedOmics datasets, and the GEPIA were used to identify the co-expression genes of SCAMP1,5 and the correlation between SCAMPs members. We conclude that SCAMPs 1 and 5 significantly represent promising diagnosis and prognostic biomarkers.

INTRODUCTION

Pancreatic cancer remains a major cause of cancer related death. Pancreatic tumors develop from the dysregulated proliferation of cells in the pancreas. Approximately 50% of cases of pancreatic cancer are diagnosed in those aged over 75. The most common type of pancreatic cancer is pancreatic ductal adenocarcinoma, the current therapies for which including surgery, chemotherapy and radiotherapy are ineffective. Due to the difficulties of treating malignant PAAD tumors, many patients have failed to receive

optimal therapeutic regimens. New and more effective diagnosis and treatments for this and other forms of pancreatic cancer are therefore urgently required.

SCAMPs function as post-Golgi transporters in all mammalian cells. The expression of the SCAMP family members differs in many cell types, with each SCAMP proposed to act during key stages of post-Golgi transport [1]. SCAMPs 1-3 possess a cytoplasmic N-terminal domain with multiple NPF (R-P-F) repeats, conserved transmembrane regions (TMs) and a cytoplasmic tail that mediates surface to Golgi transport

[2]. However, SCAMPs 4-5 differ from other family members as they lack a highly conserved cytoplasmic NPF repeat [3]. SCAMPs are integral membrane proteins that are ubiquitously expressed, most notably in secretory cells [4–6]. Although SCAMP functionality is yet to be defined, previous studies highlight their role in endocytosis, exocytosis and vesicular trafficking [7–9]. SCAMPs co-exist in circulating transport vesicles originating from post-Golgi and endocytic transport and so do not function during endosome recycling. SCAMPs therefore act at similar stages of post-Golgi function though the precise functionality of each SCAMP member remains poorly defined [9].

SCAMP1 dampens down the invasive ability of MTSS1 in triple-negative breast cancer cells through the trafficking mediated upregulation of RAC1-GTP, thus enhancing cell adhesion. The cooperative activity of MTSS1 and SCAMP1 prevents triple-negative breast cancer cell invasion whilst their silencing enhances the aggressiveness of these cancer cells [10]. We previously demonstrated that SCAMP1 silencing inhibits the metastatic phenotypes of human pancreatic and gallbladder cancer cells [11]. SCAMP1 is differentially expressed in normal vs. tumor tissue in patients with cervical cancer and pancreatic cancer lacking lymph node metastasis [11, 12].

The growth of melanoma tumors is inhibited following EFEMP1 and SCAMP3 silencing by miR-192-5p and miR-584-3p targeting, respectively. The AMPK activator Metformin also displays anti-cancer activity, particularly in cases of melanoma in which cancer cell growth is inhibited through direct effects on miR-192-5p-EFEMP1 and miR-584-3p-SCAMP3 pathways [13]. SCAMP3 also mediates inflammatory responses in breast cancer cells [14]. SCAMP4 accumulates on the surface of senescent cells and promotes SASP (The senescence-associated secretory phenotype) factor secretion, in addition to IL6, IL8, and growth differentiation factor 15 (GDF-15). Moreover, SCAMP3 promotes an SASP phenotype, a major trait of senescent cells [4]. However, knowledge of the cellular roles of SCAMP5 are limited in comparison to other family members. Unlike other SCAMP family members, neuronal SCAMP5 contributes to endocytic recycling to promote neuronal conduction [15].

In this study, we assessed cancer vs. healthy tissue and found that the expression of SCAMPs1-4 is higher in PAAD compared to normal tissue. In contrast SCAMP5 expression was downregulated in PAAD. Moreover, the expression of SCAMPs 1-4 were enhanced in *in vitro* PAAD cell lines according to online cancer databases. Our immunohistochemical analysis and HPA, GEPIA databases were used to measure the differential

expression of SCAMPs and survival analysis based on HPA, GEPIA databases which suggested that the lower SCAMP1 led to improved overall survival (OS), whilst the low levels of SCAMP5 led to a poor OS. In addition, the cBioPortal for Cancer Genomics, LinkedOmics datasets and GEPIA were used to analyze the correlation between SCAMPs 1, 4 and 5 in PAAD in which a significant correlation was identified. These data highlight SCAMPs as important diagnostic and therapeutic targets for PAAD.

RESULTS

Differential expression and diagnosis model of SCAMPs mRNA between PAAD and normal samples

According to the Gene Expression Profiling Interactive Analysis (GEPIA) datasets, an Online web-analysis tool frequently used to assess TCGA and GTEx databases, mRNA profiles of individual SCAMPs were compared between normal tissue and PAAD. The results showed that SCAMPs 1-4 were expressed to higher levels in PAAD than normal samples, whilst the opposite phenotype was observed for SCAMP5 (Figure 1A, 1C). In addition, expression violin plots showed SCAMP1 and SCAMP5 had a significant correlation with patients' pathological stage (Figure 1B). Next, ROC curves indicated that the AUC index in TCGA and GTEx datasets was 0.867($p < 0.001$), 0.890($p < 0.001$), 0.797($p < 0.001$), 0.567($p < 0.05$) and 0.913($p < 0.001$) respectively (Figure 1D). Additionally, we also found the significant difference in SCAMP1 ($p < 0.05$) and SCAMP5 ($p < 0.05$) between early stage (Stage I + II) and late stages (Stage III + IV) as diagnosis markers. (Supplementary Figure 1A, 1B) Because the sample size of PAAD in Stage III + IV is small, we also calculated the difference in SCAMP1 ($p > 0.05$) and SCAMP5 ($p < 0.05$) between early stages (Stage I + II a) and late stages (Stage II b + III + IV) (Supplementary Figure 1C, 1D).

Expression of SCAMPs in PAAD cells

Using the Cancer Cell Line Encyclopedia (CCLE) database and the bubble heatmap visualizer derived from the GTEx-Portal, gene expression data was visualized from the datasets. Upon the assessment of an array of cancer cell lines, SCAMPs 1-4 were highly expressed, but SCAMP5 was expressed to lower levels in PAAD cells (Figure 2A–2E). The European Bioinformatics Institute (EMBL-EBI) database was also used to further assess SCAMP expression in the PAAD cells. The analysis confirmed that SCAMPs1-4 were overexpressed in the majority of PAAD lines, whilst SCAMP5 was expressed to low levels (Figure 2F).

We also validated the expression of SCAMPs in PAAD cell lines (PANC-1, SW1990 and AsPC-1 cell) and normal human pancreatic ductal cell (HPDE cell) by Real-time quantitative PCR and Western blot assay. The result showed that SCAMPs1-4 were overexpressed in PANC-1 cell; whilst SCAMP5 was expressed to low levels in AsPC-1 cell line (Figure 2G–2I).

Prognostic analysis of the SCAMPs in PAAD

We next performed survival analysis for SCAMPs 1-5 using the Human Protein Atlas (HPA) and GEPIA databases in PAAD. The data showed that SCAMPs 1,5 were strongly associated with a poor OS in PAAD from both databases (Figure 3A, 3B).

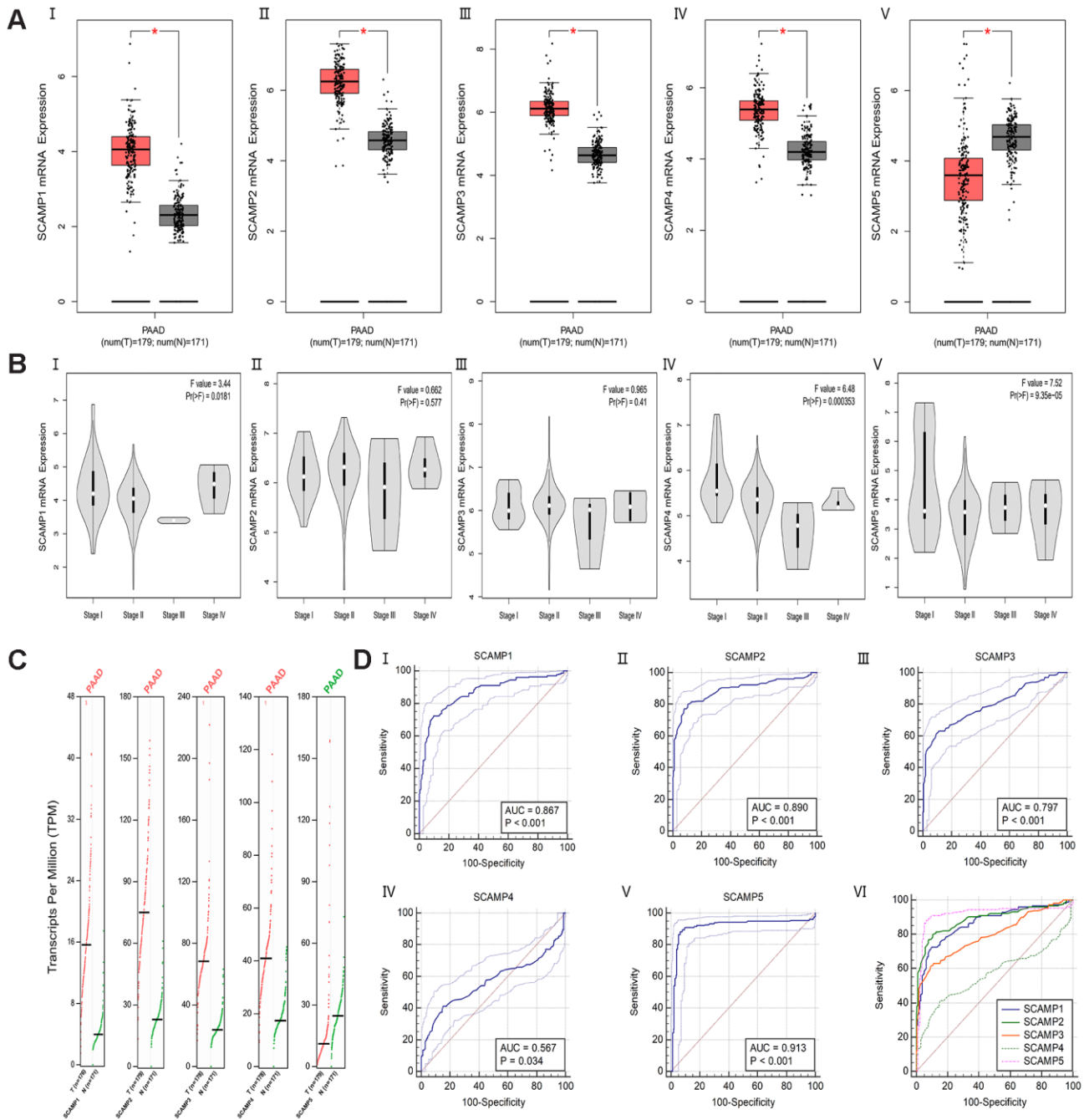


Figure 1. Differential expression and ROC curves of SCAMPs in PAAD. (A) Differential expression of SCAMP 1-5 (I-V) in PAAD ($\log_2(\text{TPM} + 1)$). (B) Expression violin plots of SCAMP 1-5 (I-V) based on patient pathological stage ($\log_2(\text{TPM} + 1)$). (C) Differential expression of SCAMP 1-5 in PAAD (TPM). (D) The Area Under the Curve (AUC) metrics are also provided for SCAMP1-5 (I-V) to predict diagnosis in PAAD by Medcalc (version 19.0); the comparison of ROC curves for SCAMP1-5 (VI).

SCAMP5 downregulation was associated with poor OS in PAAD (Figure 3A, 3B) whilst SCAMP1 overexpression led to a poor prognosis, suggesting its role as an oncogene. Thus, both SCAMPs 1, 5 act as predictors for the diagnosis and prognosis of PAAD.

SCAMP1 and SCAMP5 expression and their correlation with the clinicopathological characteristics and prognosis of PAAD

We used immunohistochemistry to assess the expression of SCAMP 1, 5 in 238 paraffin-embedded PAAD

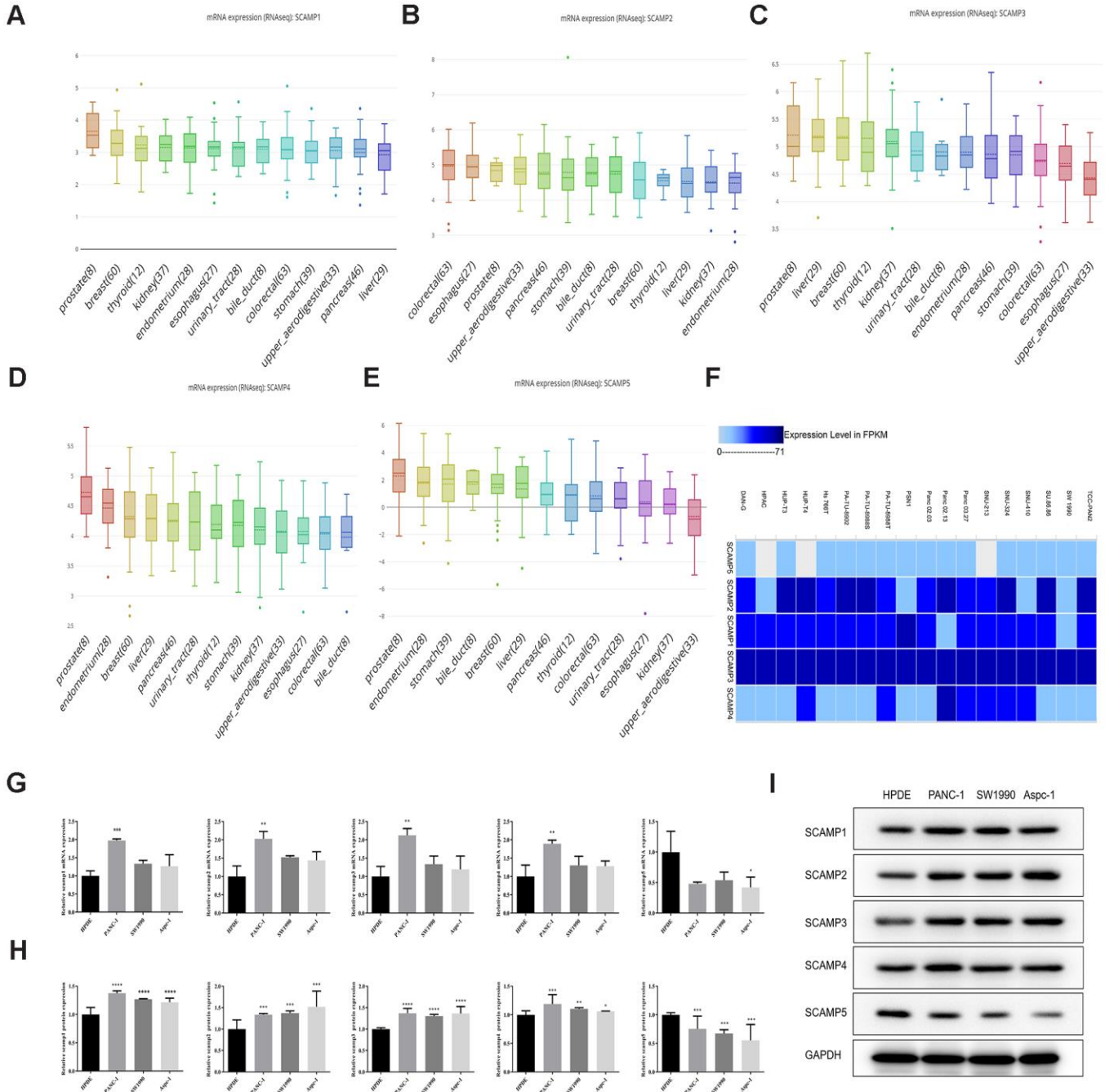


Figure 2. Expression of SCAMPs in PAAD cell lines using CCLE and the EMBL-EBI: Expression Atlas. (A–E) Expression of SCAMPs in PAAD cell lines using the CCLE database. **(F)** Expression of SCAMPs in PAAD cell lines using the EMBL-EBI (Expression Atlas) database. **(G–I)** The verification of SCAMPs expression was evaluated by RT-qPCR **(G)** and western blotting **(H, I)** in PAAD cell lines (PANC-1, SW1990 and AsPC-1 cell) and normal human pancreatic ductal cell (HPDE cell). Results shown are the mean \pm SD (* $p < 0.05$, ** $p < 0.01$, *** $p < 0.001$).

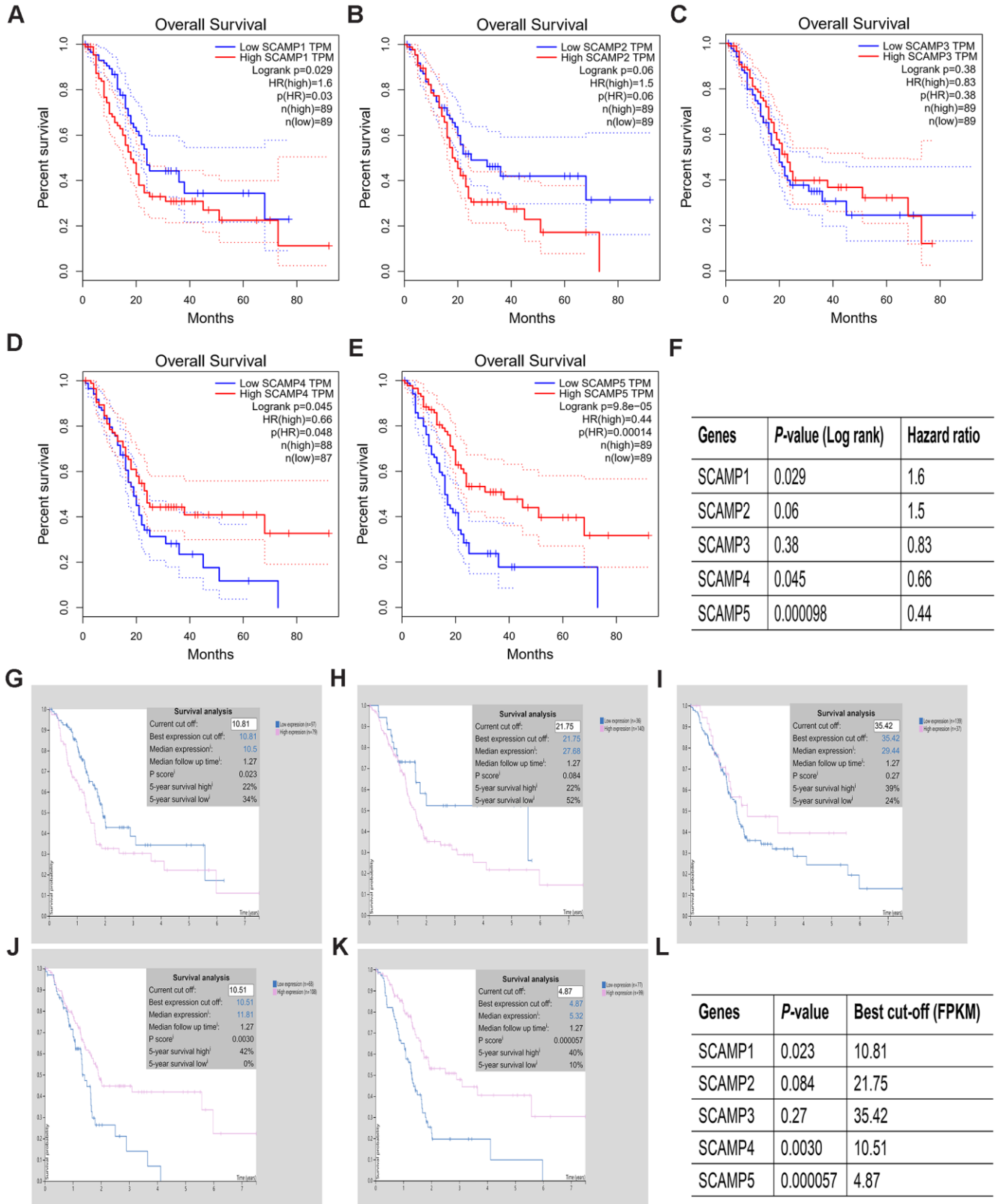


Figure 3. Prognostic value of SCAMP expression in PAAD patients (HPA and GEPIA). (A–L). Prognostic value of SCAMP expression in PAAD patients according to GEPIA (A–F) and HPA (G–L) databases.

and 117 adjacent normal specimens. Immunostaining for SCAMP1,5 was mostly cytoplasmic/membranous in PAAD cells (Figure 4A, 4B). Upon analysis of SCAMP1,5 expression with clinicopathologic parameters, SCAMP1 overexpression positively correlated with age, N stage, TNM stage and Neural invasion, whilst the down-regulation of SCAMP5 correlated with age, T stage, N stage, TNM stage and pathology differentiation (Table 1). Kaplan–Meier survival plots showed that higher SCAMP1 or lower SCAMP5 expression correlated with poorer prognosis in PAAD patients (log-rank test, $p=0.020$; $p=0.004$, Figure 4C, 4D). Moreover, univariate analysis indicated that age, metastasis, SCAMP1 expression and SCAMP5 expression were significantly associated with the risk of cancer-related death. Multivariate analysis showed that SCAMP1 and SCAMP5 expression were independent prognostic factors (Table 2). Chi-Square tests were used to investigate SCAMP1, 5 expression in adjacent normal and pancreatic adenocarcinoma ($p<0.0001$), (Figure 4E, 4F).

SCAMP correlation analysis

The cBioPortal for Cancer Genomics was used to analyze the co-expression of SCAMPs1, 5 from 179 PAAD tumors. The most significant genes that correlated with SCAMPs 1 and 5 (Figure 5A) were TMED7 (positive Spearman's Correlation=0.742 $p<0.001$), DAZAP1 (negative Spearman's Correlation=-0.673 $p<0.001$) and BEX1 (positive Spearman's Correlation= 0.786 $p<0.001$) and TGIF1 (negative Spearman's Correlation= -0.572 $p<0.001$). Other identified genes are summarized in Supplementary Table 1. Using the LinkedOmics database, SCAMP1 was found to negatively correlate with SCAMP 3 (spearman correlation: -0.4085, $p < 0.01$), whilst SCAMP3 positively correlated with SCAMP4 (spearman correlation: 0.3489, $p < 0.0001$) (Figure 5B, 5C). These data were verified in the GEPIA datasets in which SCAMP1 correlated with SCAMP2 ($R: 0.31$, $p < 0.05$), whilst SCAMP3 correlated with SCAMP4 ($R: 0.37$, $p < 0.05$), (Figure 5D, 5E) in PAAD samples.

Functional enrichment analysis of SCAMPs 1, 4 and 5

GO and KEGG pathway analysis of SCAMPs 1, 4 and 5 were performed to shed further light on their biological functions. GO term analysis in GSEA showed that the SCAMPs associated with the ribosomes (SCAMPs 1-4) and condensed chromosomes (SCAMP5) were they participate translational initiation (SCAMPs 1 and 4) or chromosome segregation (SCAMP 5). Furthermore, the SCAMPs were shown to participate in the structural constituent of ribosomes (SCAMPs 1 and 4) and cell adhesion molecule binding (SCAMP5) (Figure 6A–6C).

KEGG pathway analysis showed enrichment in the ribosomes (SCAMPs 1 and 4) and cell cycle components (SCAMP 5) (Figure 6A–6C).

Establishment and analysis of the PPI/ functional network

We firstly constructed PPI network of SCAMPs family by the predicted mode of molecular action, and constructed a two-layered model to reveal the regulatory networks of the SCAMPs in PAAD using GeneMania. The outer layer included genes co-expressed and interacting with PLD1, ATP5L, PLD2, SYT2, EGFR, ST3GAL3, SYNRG, BCAP31, ITSN1, RAB2A, SNAP23, FAM189B, REEP5, UNC93B1, JAGN1, EPS15, BAG6, SNRPD1, ARF6, and SNRPD3 (Figure 7).

DISCUSSION

The dysregulation of SCAMPs occurs frequently in an array of cancers [10–16]. This study explored the differential expression and prognostic value of SCAMPs in PAAD in an attempt to improve PAAD treatment and diagnostic accuracy.

Emerging studies suggest that the dysregulation of SCAMP1 is related to the occurrence and progression of various tumors, including pancreatic cancer, gallbladder cancer, cervical cancer and breast cancer [10–12]. The downregulation of SCAMP1 suppresses the migration and invasion of tumor cells [11, 17]. SCAMP1 upregulates VEGF secretion that is required for nutrient support for newly formed blood vessels [18]. SCAMP1 also suppresses the malignant proliferation of glioma cells through the miR-499a-5p/LMX1A/NLRC5 axis, highlighting SCAMP1 as an oncogene [19]. SCAMP1 is a key cellular regulator of endocytic and secretory pathways through its dual role in the stimulation of dilation and blocking fusion pores, which downregulates bulk exocytosis [20]. In this study, the aforementioned cancer databases demonstrated that SCAMP1 expression is elevated in PAAD vs. healthy tissue. These findings were confirmed following the assessment of SCAMP1 levels in a range of *in vitro* PAAD culture systems, in which SCAMP1 was significantly elevated compared to non-cancerous pancreatic cell lines. Combining GEPIA and HPA datasets with our clinical data revealed that SCAMP1 provides strong prognostic value in PAAD patients. Upregulated SCAMP1 significantly correlated with poor OS.

We found that the expression of SCAMPs 2 and 3 in PAAD samples were higher than normal pancreatic samples. SCAMP 2 and 3 expression were also elevated

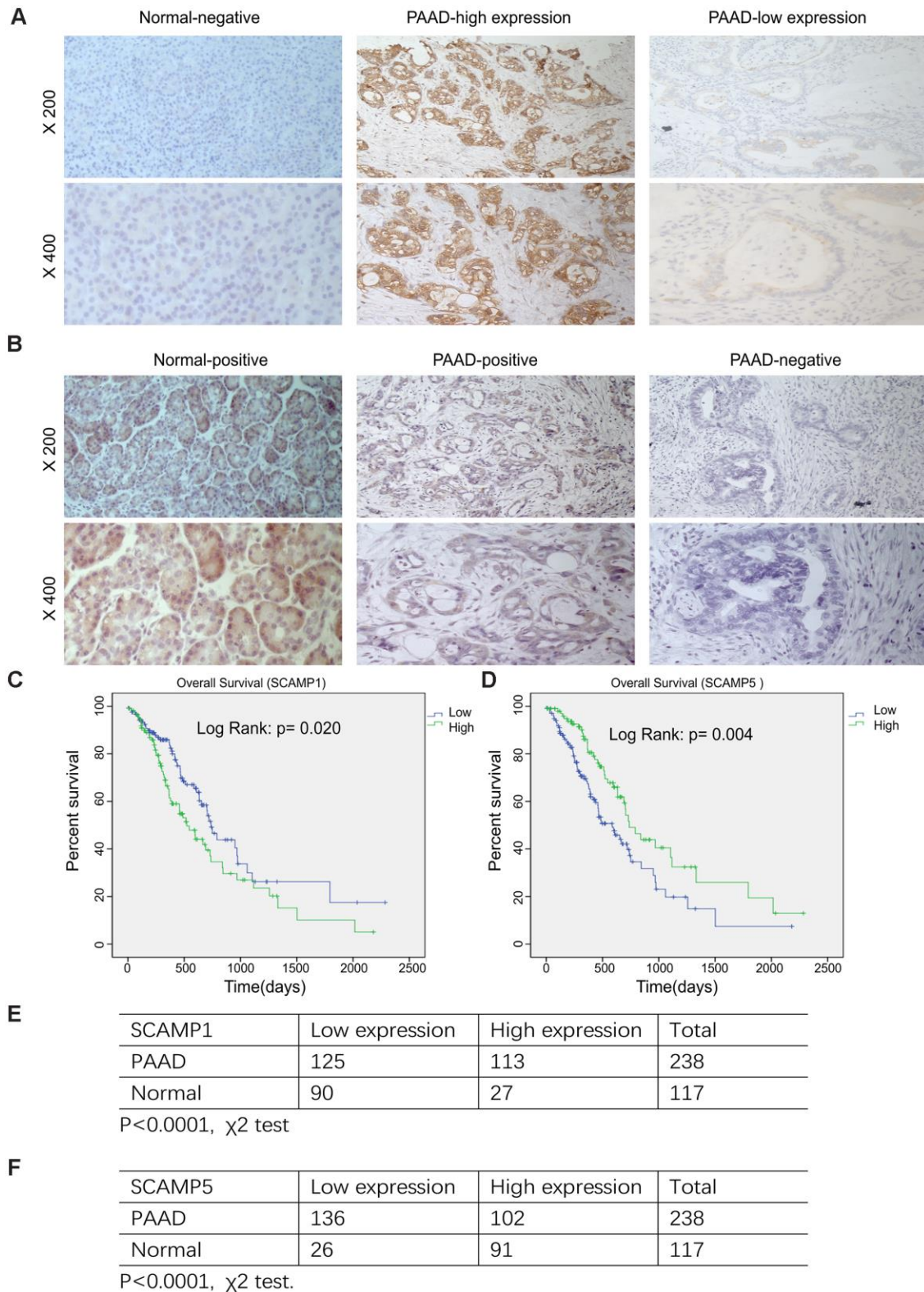


Figure 4. Relationship SCAMP1, 5 expression and the clinicopathological parameters of PAAD patients. (A, B) Representative images of SCAMP1 and SCAMP5 staining in PAAD tissue. (Expression of SCAMP1 and SCAMP5 were evaluated semi-quantitatively based on staining intensity and cell positivity, representative images are shown at $\times 200$ and $\times 400$ magnification, respectively.) (C, D) Kaplan–Meier analysis of the overall survival of PAAD patients stratified by the SCAMP1 and SCAMP5 immunoreactive scores by SPSS version 19.0. Log-rank test were performed to compare differences between groups. (E, F) Quantification of SCAMP1, 5 expression in pancreatic cancer and adjacent normal samples. Statistical analyses were performed using the χ^2 test. Low: low expression, High: high expression.

Table 1. Relationship between SCAMP1, 5 expression and the clinicopathological parameters of patients with PAAD.

Characteristics	Number of cases	SCAMP1 level			SCAMP5 level		
		L	H	P value	L	H	P value
Total cases	238						
Sex							
Male	128	64	64	0.401	74	54	0.822
Female	110	61	49		62	48	
Age							
<60	91	56	35	0.028	43	48	0.015
≥60	147	69	78		93	54	
Pathology differentiation							
High (Middle or High)	175	96	79	0.229	89	86	0.001
Low (No or Low)	63	29	34		47	16	
T classification							
T1-2	44	27	17	0.193	17	27	0.006
T3-4	194	98	96		119	75	
N classification							
N0	101	67	34	0.0002	50	51	0.041
N1-2	137	58	79		86	51	
Metastasis							
No	231	122	109	0.892	133	98	0.698
Yes	7	3	4		3	4	
TNM stage							
I-IIA	96	65	31	0.0001	47	49	0.036
IIB-IV	142	60	82		89	53	
Vascular invasion							
No	172	97	75	0.053	97	75	0.707
Yes	66	28	38		39	27	
Neural invasion							
No	152	88	64	0.027	85	67	0.613
Yes	86	37	49		51	35	

Patients were staged in accordance with the 8th Edition of the AJCC Cancer's' TNM Classification. Chi-square test, numbers in bold indicate significant p-values (p<0.05). H: high, L: low.

Table 2. Univariate and multivariate Univariate cox regression models for overall survival in PAAD patients (n = 238).

Characteristics	Univariate analysis			Multivariate analysis		
	HR	95%CI	P value	HR	95%CI	P value
Age	1.670	1.101-2.534	0.016	1.398	1.033-2.420	0.131
TNM stage	1.149	0.769-1.717	0.498	0.395	0.101-2.791	0.272
T classification	1.128	0.698-1.823	0.622	0.990	0.646-1.905	0.971
N classification	1.240	0.834-1.844	0.287	2.211	0.358-9.151	0.333
Metastasis	0.956	0.348-2.621	0.029	1.556	0.320-3.324	0.468
SCAMP1	1.565	1.068-2.294	0.022	1.654	1.005-2.266	0.017
SCAMP5	0.564	0.380-0.838	0.005	0.531	0.377-0.872	0.004

Numbers in bold indicate significant p-values (p<0.05).

in human PAAD cell lines according to CCLE and EMBL-EBI databases. No positive correlation was observed between SCAMPs 2 and 3 and OS in PAAD. To-date the role of SCAMP2 in cancer is poorly

defined. SCAMP2 also colocalized with fusion sites and enhanced granule exocytosis mediated through E peptide-containing domains that inhibit exocytosis [7]. Together, these data suggest that SCAMP2 promotes

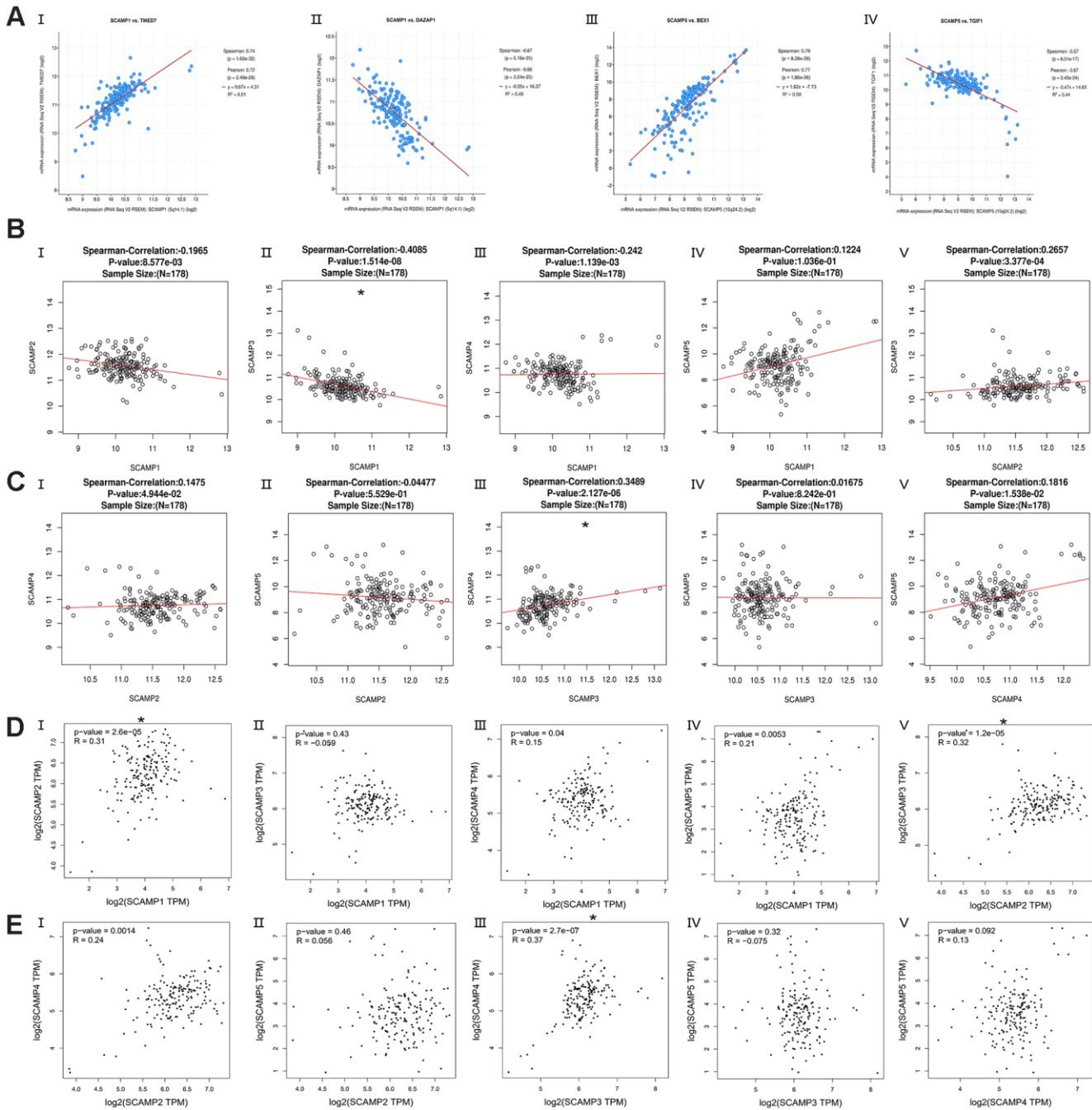


Figure 5. Co-expressed genes of SCAMP1, 5, and correction between SCAMP1- 5 in PAAD (cBioPortal for Cancer Genomics, LinkedOmics, and GEPIA). (A) Co-expressed genes (top-1) of SCAMP1, 5 in PAAD using the cBioPortal for Cancer Genomics. (I: TMED7, II: DAZAP1, III: BEX1, IV: TGIF1) (B, C) Correction between SCAMP1- 5 in PAAD using LinkedOmics. (B: I: SCAMP1 vs 2, II: SCAMP1 vs 3 III: SCAMP1 vs 4, IV: SCAMP1 vs 5, V: SCAMP2 vs 3; C: I: SCAMP2 vs 4, II: SCAMP2 vs 5 III: SCAMP3 vs 4, IV: SCAMP3 vs 5, V: SCAMP4 vs 5). (D, E) Correction between SCAMP1- 5 in PAAD using GEPIA. (R: Spearman correlation analysis; B: I: SCAMP1 vs 2, II: SCAMP1 vs 3 III: SCAMP1 vs 4, IV: SCAMP1 vs 5, V: SCAMP2 vs 3; C: I: SCAMP2 vs 4, II: SCAMP2 vs 5 III: SCAMP3 vs 4, IV: SCAMP3 vs 5, V: SCAMP4 vs 5) * Spearman correlation >0.3 or Spearman correlation <-0.3 and $p < 0.05$.

NHE5 transport through recycling endosomes and enhances its cell-surface targeting in an Arf6-dependent manner. NHE5 is a Na⁺/H⁺ exchanger enriched in brain tissue [21]. A correlation between the expression of a basic/hydrophobic peptide segment within SCAMP2: CWYRPIYKAFR that interacts with PI (4, 5) P2 and inhibits exocytosis, particularly by SC2-R204A exists.

A common electrostatic interaction is known to occur between PI (4, 5) P2 and the E peptides of SCAMPs 1 and 2 that regulates their interaction within the membrane interface during exocytosis. Similar interactions involving other SCAMPs may also exist but as yet remain undefined [22]. SCAMP2 also regulates exocytosis through other methods [23].

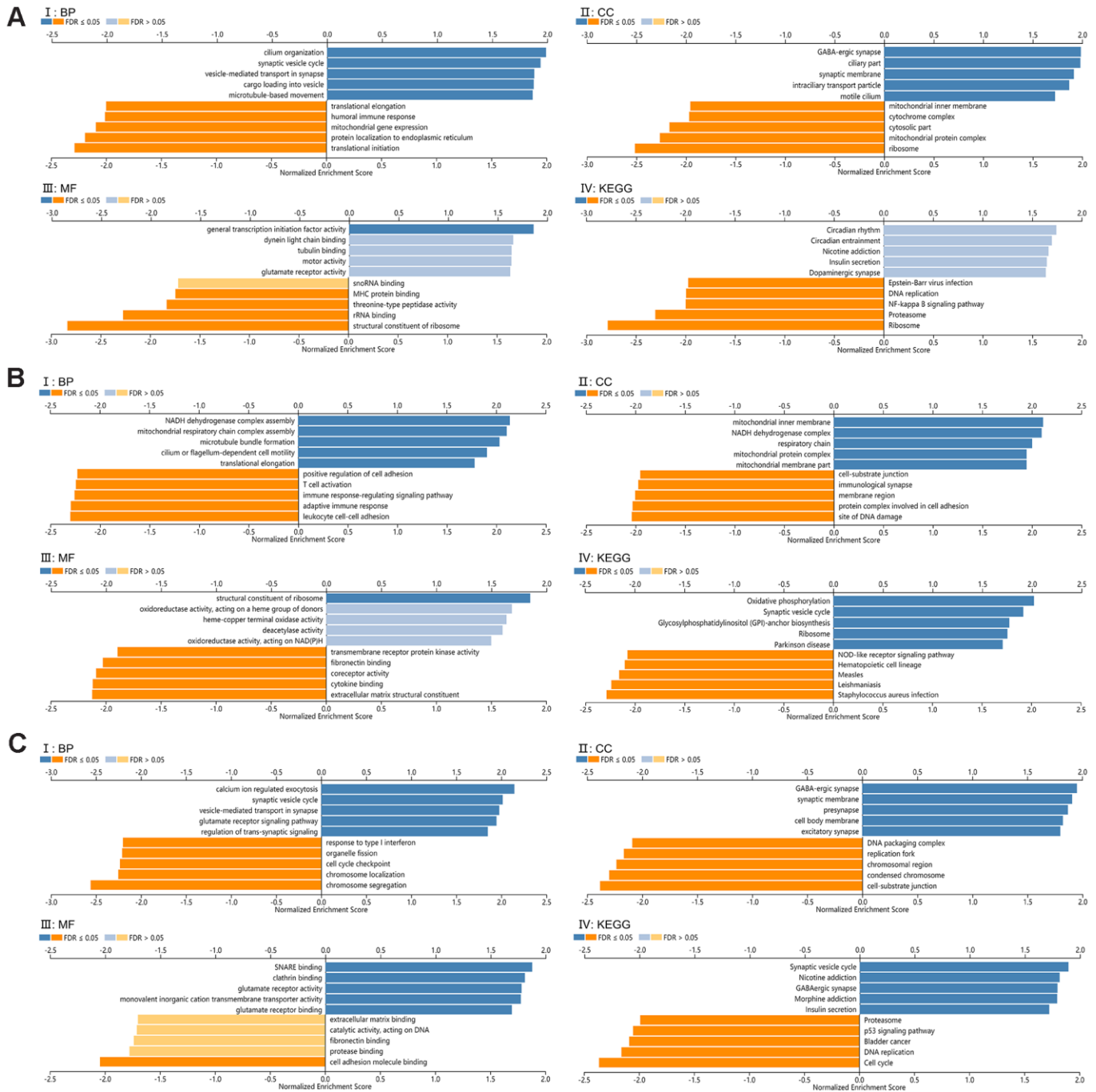
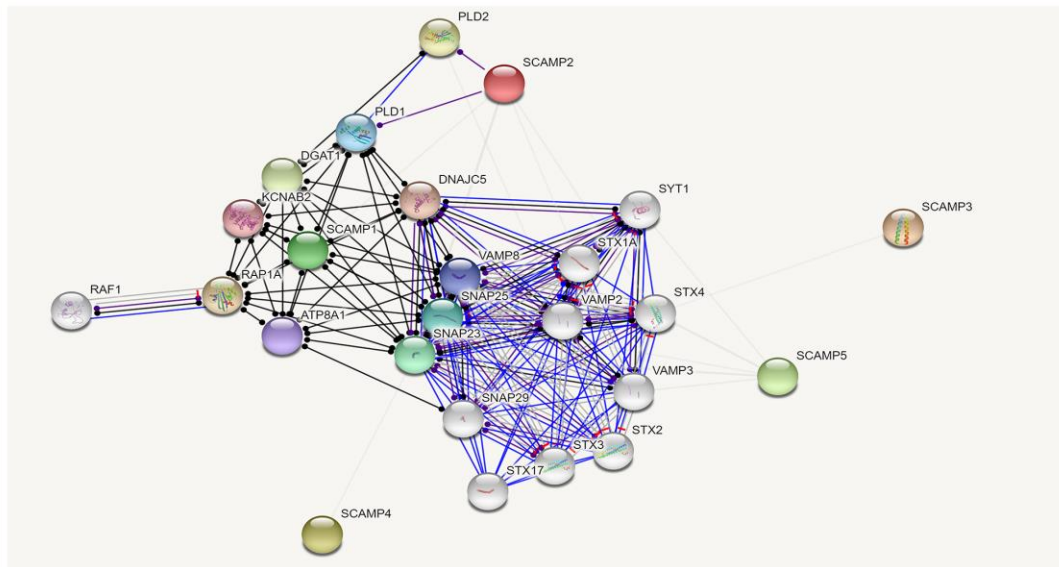


Figure 6. Functional enrichment analysis for SCAMP1, 4, 5. (A–C) Gene set enrichment analysis (GSEA) GO and KEGG pathway analysis for SCAMP1(A), 4(B), 5(C) respectively, (CC): Cellular components. (BP): Biological processes. (MF): Molecular functions. (KEGG): KEGG pathway analysis. (I: BP, II: CC, III: MF, IV: KEGG).

A



B

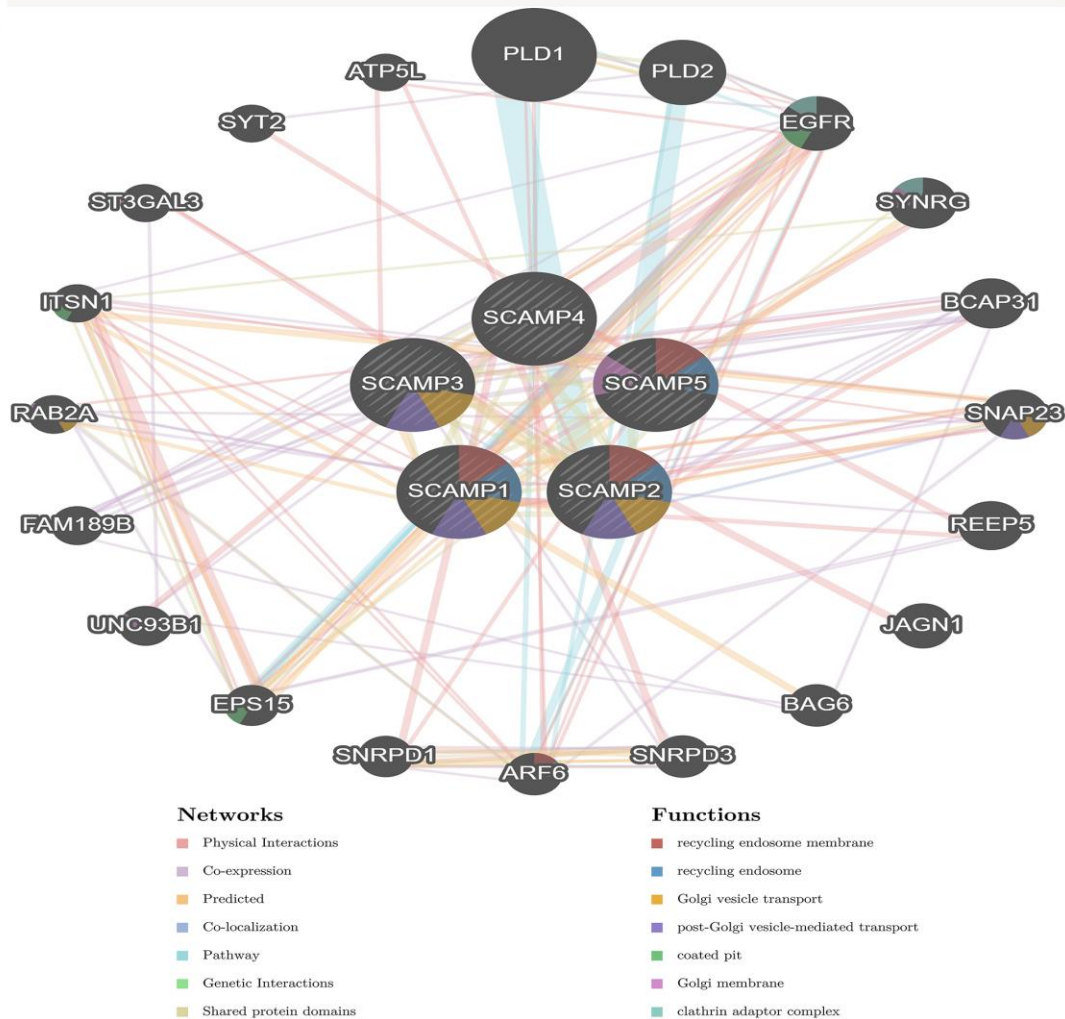


Figure 7. Protein-protein interaction network of SCAMPs (STRING, GeneMANIA). (A) Functional protein association networks of SCAMPs. Line shape indicated the predicted mode of molecular action. (B) Networks between predicted genes and SCAMP1-5. Different colors of the network edge indicate the bioinformatics methods applied: co-expression, website prediction, pathway, physical interactions and co-localization. Different colors for the network nodes indicate the biological functions of enrichment genes.

It was recently suggested that SCAMP3 acts as a prognostic biomarker and treatment target in HCC, the silencing of which suppresses HCC proliferation and cell cycle progression [16]. SCAMP3 inhibits endocytosis and receptor degradation through its ability to inhibit the ubiquitination of ESCRTs (Endosomal Sorting Complex Required for Transports) [24]. SCAMP3 positively influences the sorting and budding of intraluminal vesicles controlling multivesicular endosome biogenesis [25]. Multivesicular bodies (MVBs) regulate cell cycle progression and tumor biogenesis. Chmp1A, an ESCRT protein, inhibits cancer cell proliferation, invasion and signaling activity via MVB formation [26], highlighting the potential role of SCAMP3 during cancer development. In our analysis, SCAMP3 expression was minimally associated with the OS of PAAD patients.

The enhanced phosphorylation of PKC by SCAMP-4 alters vesicular transport [27]. SCAMP5 enhances the secretion of calcium-regulated signal peptide-containing cytokine (CL5) but not IL-1 β in MCF-7 epithelial cells [28]. SCAMP5 co-operates with SNAREs to enhance cytokine exocytosis through a process mediated by enhanced Ca²⁺ influx [28]. The role of SCAMPs 4-5 in tumor cells are less well-studied. Our data suggest that SCAMP4 is overexpressed in PAAD vs normal tissues, whilst SCAMP5 shows an opposite phenotype. Surprisingly, elevated levels of SCAMP5 correlate with an improved OS in PAAD patients. This highlights the tumor suppressive role of SCAMP5 in PAAD cells.

We next assessed the utility of SCAMPs as prognostic indicators of PAAD, to reveal important information on the molecular roles of these trafficking proteins in the development and progression of PAAD. We found that SCAMPs 1 and 5 showed dysregulated expression in PAAD tumors and play an important role in PAAD tumorigenesis, serving as molecular markers for those at an elevated risk of PAAD tumorigenesis. These data also highlighted SCAMPs 1 and 5 as potential targets for PAAD treatment, the regulation of which could improve PAAD survival and prognosis. SCAMP 1, 5 expression were significantly associated with age, N classification and TNM-stage. Enrichment analysis suggested that the functional network of SCAMPs were involved in the structural constituents of ribosomes and cell adhesion molecule binding. We further highlighted key gene members in the functional activity of the SCAMPs including PLD1, ATP5L, PLD2, SYT2, EGFR, ST3GAL3, SYNRG, BCAP31, ITSN1, RAB2A, SNAP23, FAM189B, REEP5, UNC93B1, JAGN1, EPS15, BAG6, SNRPD1, ARF6, and SNRPD3. Amongst them, PLD1, EGFR, ST3GAL3 and ARF6 mediate the progression of pancreatic cancer [29–33].

Overall, this study reveals that all SCAMP family members are differentially expressed between PAAD and normal tissues, and that SCAMPs 1, 5 may act as predictors for the diagnosis and prognosis of PAAD. SCAMPs therefore represent potential therapeutic targets for PAAD and mediate its occurrence and progression of PAAD, as in other cancers. This study still had some limitations: Firstly, our SCAMP data were obtained from public databases and verification queues only included SCAMP protein expression levels without confirmation *in vitro* or *in vivo*. Secondly, diagnosis and prognosis require extensive external verification of the clinical sample data and our diagnosis model is from tissue samples without blood or exosome samples. Thirdly, specific functional regulatory networks cannot be built without amount experiments by only bioinformatics analysis. Further studies are therefore required to verify the role played by SCAMPs in PAAD.

MATERIALS AND METHODS

Patients and tissue specimens

Pancreatic adenocarcinoma tissues were obtained from patients admitted to the Northern Jiangsu People's Hospital who had surgical abscission treatment from October 2015 to October 2019. Patients were individually diagnosed by 2 pathologists, had not received chemotherapy or radiation therapy prior to surgical procedures. A total of 238 cancerous and 117 noncancerous paraffin-embedded specimens were used for immunohistochemistry analysis.

Real-time quantitative PCR and western blot assay

Shanghai Institute of Nutrition and Health in Shanghai, China provided the human PAAD cell lines PANC-1, SW1990, AsPC-1, and normal HPDE cell (Human pancreatic ductal cell). A one percent strength streptomycin-penicillin along with fetal bovine serum of ten percent strength was part of the medium in which the cells were cultured at a temperature of 37° C and five percent carbon dioxide- fed humidified incubator.

The Trizol reagent (from Invitrogen, (China) was used to extract the total ribonucleic acid while the PT-PCR Kit sourced from Vazyme (China) was used to reverse transcribe the samples. The primers used in this study were: SCAMP1- forward: 5'-TTCGACAGTAACCCGTTTGC-3'; SCAMP1- reverse: 5'-ATTAGGCATCTT CACACCGC-3'; SCAMP2- forward: 5'-CAGAGATC CCTGCCGACTAC-3'; SCAMP2- reverse: 5'-CAGGC AAGCAGGTTTCAGAAA-3'; SCAMP3- forward: 5'-A TCCACTCCTTATACCGCCG-3'; SCAMP3- reverse: 5'-GAGAAGACACCAGCAGCAAA-3'; SCAMP4-

forward: 5'-TTCCGGCCTGTCTACAAGG-3'; SCAMP4- reverse: 5'-AACTGGGCTCCGAAGATGAA-3'; SCAMP5- forward: 5'-ACCAAGACTTCGAGGCA GAT-3'; SCAMP5- reverse: 5'-CGCTGTTCAACATC CAGAGG-3'; C3H6O3 (Glyceraldehyde) -3-G6PD_N (phosphate dehydrogenase): forward: 5'-GGTGAAGG TCGGAGTCAACG-3'; reverse: 5'-CAAAGTTGTCA TGGATGACC-3'. GAPDH Ct was the value to which each Ct value expression was normalized to determine relative expressions. RT-qPCRs were performed as the MIQE (Minimum Information for Publication of Quantitative Real-Time PCR Experiments) guidelines [34].

RIPA (from Solarbio (China) was used to lyse the cells. The radioimmunoprecipitation assay contained a protease inhibitor maintained on ice for thirty minutes. A five percent mixture of bovine serum albumin from Invitrogen (China) was used to block the membranes and incubation was done overnight at 4° C. Subsequently, for a duration of 1 h, incubation was conducted using horseradish peroxidase (HRP)-conjugated goat anti-mouse or goat anti-rabbit sourced from Cell Signaling Technology, China. SCAMP1, SCAMP2, SCAMP3, SCAMP4 and SCAMP5 antibodies sourced from proteintech, China was used to perform western blot assay with anti-GAPDH antibody (Abcam) as a loading control. Data was analyzed by GraphPad Prism 8.0 (GraphPad Software Inc., San Diego, CA) and presented as mean ± SD. One-way analysis of variance (ANOVA) followed Tukey's test was employed to compare differences among multiple groups. $P < 0.05$ was indicated as statistically significant.

Immunohistochemistry

The sample was blocked and incubated with the SCAMP1, 5 Ab (1: 50) for 2 hours at 23° C, and an HRP conjugated goat anti-rabbit Ab was used as the secondary probe. 2 pathologists, independent of each other and blinded by the patients' clinical data gave the evaluation of immunohistochemical staining. SCAMP1, 5 expression levels were classified by the semi-quantitative method that combines the intensity of the staining as well as the percentage of cells that stained positive. [35, 36]

GEPIA datasets

GEPIA is an online analysis tool that provides a python package for the rapid analysis and retrieval of data based on TCGA and GTEx datasets. The database provides an interactive and customizable function including differential expression analysis, profiling plots, correlation analysis, survival analysis, gene

analysis, and dimensionality reduction [37]. We used log-rank tests (Mantel–Cox tests) for hypothesis evaluation and selected the Cox proportional hazard ratio and 95% confidence interval for survival analysis.

LinkedOmics datasets

LinkedOmics can compare multi-omic cancer datasets across an array of tumor types (32 cancers and 11,158 patients) from the TCGA project and proteomics data from the CPTAC. LinkedOmics contains three key analysis modules: namely LinkFinder, LinkCompare, and LinkInterpreter, and displays data in the form of volcano plots, heat maps, or scatter plots [36]. The LinkInterpreter module builds statistical plots for individual genes and performs pathway and functional network analyses of differentially expressed genes (DEGs). This comprehensive, flexible and interactive functional category database provides an online gene set analysis toolkit (WebGestalt) which was applied in this study [38, 39]. LinkedOmics was used to sign and rank the data from the LinkFinder, which was selected for GSEA to perform GO (BP, CC and MF), and KEGG analysis. We used non-parametric analysis and Pearson Correlation tests to obtain our data. Criterion were ranked with an FDR < 0.05. A total of 500 simulations were performed.

CCLE datasets

The CCLE is an amalgamation of copy number data, gene expression analysis, and parallel sequencing assessments from 947 human cancer cell lines formed by the Broad and Novartis Institutes for Biomedical Research and the Genomics Institute of the Novartis Research Foundation. The CCLE can be used for the assessment of cell targets, gene variants, small-molecules and therapeutics, permitting the identification of novel marker-driven cancer dependencies. The CCLE datasets and their accompanying public data portals provide a resource to promote cancer research using model *in vitro* cancer cell lines [40–43]. SCAMP expression in cancer cell lines can be verified using the CCLE dataset.

EMBL-EBI (expression atlas) dataset

The expression Atlas was used to verify SCAMP expression in the PAAD cell lines. EMBL-EBI is a continually updated database that provides gene and protein expression data in an array of species and contexts, including tissue development, diseases and cell types. The expression Atlas includes 1101 studies on human microarrays and RNA-sequencing data from Blueprint, PCAWG, ENCODE, GTEx and HipSci databases [44, 45].

HPA datasets

HPA acts as a roadmap for all human protein-protein interactions through its integration of antibody-based imaging, mass spectrometry-based proteomics, transcriptomics and systems biology, thus providing an interactive web-based tool to explore gene expression and survival in 17 cancer types. The Tissue Atlas and Human Pathology Atlas characterize the expression and localization of human proteins in various tissues and organs according to RNA-seq, immunohistochemistry of tissue microarrays and transcriptomes using data from ≥ 8000 patients [46–48].

cBioPortal for cancer genomics

The cBioPortal for Cancer Genomics is an open platform that permits the interactive exploration of multidimensional cancer genomic datasets. The cBioPortal allows researchers to convert complex genomic data into visual biological insights and clinical applications including somatic mutations, DNA copy-number alterations (CNAs), mRNA and microRNA (miRNA) expression, DNA methylation, protein expression and phosphoprotein levels [49, 50].

STRING and GeneMANIA

Search Tool for the Retrieval of Interacting Genes (STRING; <http://string-db.org>) (version 11.0) database can provide the analysis of functional interactions between proteins, and provide insights for the research on the mechanism of disease occurrence or progression [51]. Co-expressed genes that co-localize or interact either directly or with the targets of SCAMPs were identified using GeneMania. The database encompasses data from the GEO, physical and genetic interaction data from BioGRID and predicted protein interactions based on orthology from I2D. Pathways and molecular interaction data were derived from the Pathway Commons [52]. SCAMPs and their functional networks in PAAD were analyzed using this STRING and GeneMania.

AUTHOR CONTRIBUTIONS

FM conceived and designed this study. The clinical tissue specimens were collected by FM, AA and ZX. The experiments and the data analyses were carried out by FM and HD. Other authors including YD, NL, XW, and JQ also participated in the data analyses of this study. The manuscript was written by FM and supervised by JY. All authors read and approved the manuscript and agree to be accountable for all aspects of the research in ensuring that the accuracy or integrity of any part of the work was appropriately investigated and resolved.

CONFLICTS OF INTEREST

The authors declare that they have no conflicts of interest.

FUNDING

This work was supported by a grant from the National Natural Science Foundation of China (No. 81772516).

REFERENCES

1. O'Leary NA, Wright MW, Brister JR, Ciuffo S, Haddad D, McVeigh R, Rajput B, Robbertse B, Smith-White B, Ako-Adjei D, Astashyn A, Badretdin A, Bao Y, et al. Reference sequence (RefSeq) database at NCBI: current status, taxonomic expansion, and functional annotation. *Nucleic Acids Res.* 2016; 44:D733–45. <https://doi.org/10.1093/nar/gkv1189> PMID:[26553804](https://pubmed.ncbi.nlm.nih.gov/26553804/)
2. Castle A, Castle D. Ubiquitously expressed secretory carrier membrane proteins (SCAMPs) 1-4 mark different pathways and exhibit limited constitutive trafficking to and from the cell surface. *J Cell Sci.* 2005; 118:3769–80. <https://doi.org/10.1242/jcs.02503> PMID:[16105885](https://pubmed.ncbi.nlm.nih.gov/16105885/)
3. Kim KM, Noh JH, Bodogai M, Martindale JL, Pandey PR, Yang X, Biragyn A, Abdelmohsen K, Gorospe M. SCAMP4 enhances the senescent cell secretome. *Genes Dev.* 2018; 32:909–14. <https://doi.org/10.1101/gad.313270.118> PMID:[29967290](https://pubmed.ncbi.nlm.nih.gov/29967290/)
4. Brand SH, Laurie SM, Mixon MB, Castle JD. Secretory carrier membrane proteins 31-35 define a common protein composition among secretory carrier membranes. *J Biol Chem.* 1991; 266:18949–57. PMID:[1717458](https://pubmed.ncbi.nlm.nih.gov/1717458/)
5. Laurie SM, Cain CC, Lienhard GE, Castle JD. The glucose transporter GluT4 and secretory carrier membrane proteins (SCAMPs) colocalize in rat adipocytes and partially segregate during insulin stimulation. *J Biol Chem.* 1993; 268:19110–17. PMID:[8360193](https://pubmed.ncbi.nlm.nih.gov/8360193/)
6. Law AH, Chow CM, Jiang L. Secretory carrier membrane proteins. *Protoplasma.* 2012; 249:269–83. <https://doi.org/10.1007/s00709-011-0295-0> PMID:[21633931](https://pubmed.ncbi.nlm.nih.gov/21633931/)
7. Liu L, Guo Z, Tieu Q, Castle A, Castle D. Role of secretory carrier membrane protein SCAMP2 in granule exocytosis. *Mol Biol Cell.* 2002; 13:4266–78. <https://doi.org/10.1091/mbc.e02-03-0136> PMID:[12475951](https://pubmed.ncbi.nlm.nih.gov/12475951/)

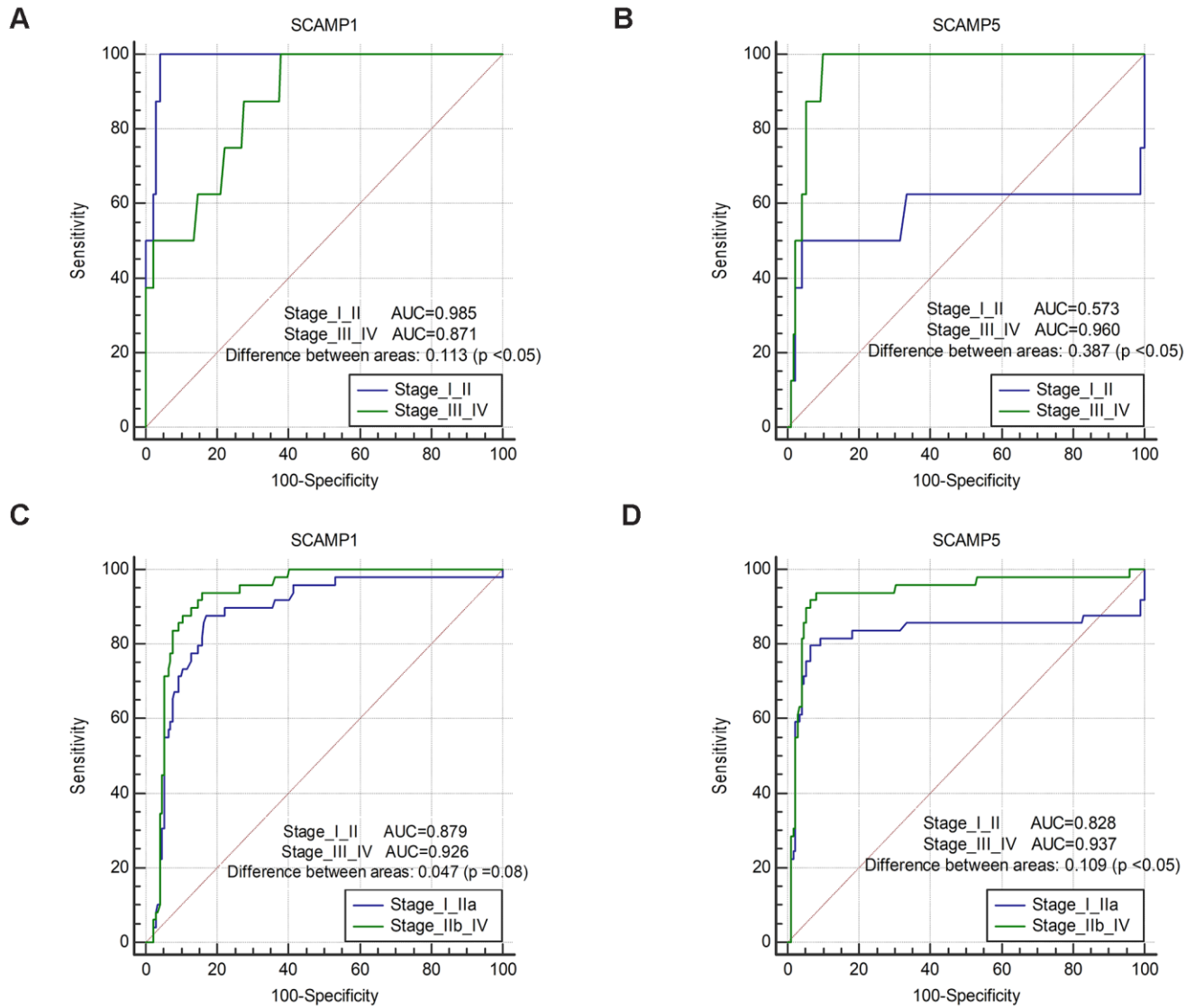
8. Guo Z, Liu L, Cafiso D, Castle D. Perturbation of a very late step of regulated exocytosis by a secretory carrier membrane protein (SCAMP2)-derived peptide. *J Biol Chem.* 2002; 277:35357–63.
<https://doi.org/10.1074/jbc.M202259200>
PMID:[12124380](https://pubmed.ncbi.nlm.nih.gov/12124380/)
9. Singleton DR, Wu TT, Castle JD. Three mammalian SCAMPs (secretory carrier membrane proteins) are highly related products of distinct genes having similar subcellular distributions. *J Cell Sci.* 1997; 110:2099–107.
PMID:[9378760](https://pubmed.ncbi.nlm.nih.gov/9378760/)
10. Vadakekolathu J, Al-Juboori SI, Johnson C, Schneider A, Buczek ME, Di Biase A, Pockley AG, Ball GR, Powe DG, Regad T. MTSS1 and SCAMP1 cooperate to prevent invasion in breast cancer. *Cell Death Dis.* 2018; 9:344.
<https://doi.org/10.1038/s41419-018-0364-9>
PMID:[29497041](https://pubmed.ncbi.nlm.nih.gov/29497041/)
11. Yang S, Lee KT, Lee JY, Lee JK, Lee KH, Rhee JC. Inhibition of SCAMP1 suppresses cell migration and invasion in human pancreatic and gallbladder cancer cells. *Tumour Biol.* 2013; 34:2731–39.
<https://doi.org/10.1007/s13277-013-0825-9>
PMID:[23653380](https://pubmed.ncbi.nlm.nih.gov/23653380/)
12. Biewenga P, Buist MR, Moerland PD, Ver Loren van Themaat E, van Kampen AH, ten Kate FJ, Baas F. Gene expression in early stage cervical cancer. *Gynecol Oncol.* 2008; 108:520–26.
<https://doi.org/10.1016/j.ygyno.2007.11.024>
PMID:[18191186](https://pubmed.ncbi.nlm.nih.gov/18191186/)
13. Tseng HW, Li SC, Tsai KW. Metformin treatment suppresses melanoma cell growth and motility through modulation of microRNA expression. *Cancers (Basel).* 2019; 11:209.
<https://doi.org/10.3390/cancers11020209>
PMID:[30754729](https://pubmed.ncbi.nlm.nih.gov/30754729/)
14. Suárez-Arroyo IJ, Feliz-Mosquea YR, Pérez-Laspiur J, Arju R, Giashuddin S, Maldonado-Martínez G, Cubano LA, Schneider RJ, Martínez-Montemayor MM. The proteome signature of the inflammatory breast cancer plasma membrane identifies novel molecular markers of disease. *Am J Cancer Res.* 2016; 6:1720–40.
PMID:[27648361](https://pubmed.ncbi.nlm.nih.gov/27648361/)
15. Zhao H, Kim Y, Park J, Park D, Lee SE, Chang I, Chang S. SCAMP5 plays a critical role in synaptic vesicle endocytosis during high neuronal activity. *J Neurosci.* 2014; 34:10085–95.
<https://doi.org/10.1523/JNEUROSCI.2156-14.2014>
PMID:[25057210](https://pubmed.ncbi.nlm.nih.gov/25057210/)
16. Zhang X, Sheng J, Zhang Y, Tian Y, Zhu J, Luo N, Xiao C, Li R. Overexpression of SCAMP3 is an indicator of poor prognosis in hepatocellular carcinoma. *Oncotarget.* 2017; 8:109247–57.
<https://doi.org/10.18632/oncotarget.22665>
PMID:[29312605](https://pubmed.ncbi.nlm.nih.gov/29312605/)
17. Hanson J, Gorman J, Reese J, Fraizer G. Regulation of vascular endothelial growth factor, VEGF, gene promoter by the tumor suppressor, WT1. *Front Biosci.* 2007; 12:2279–90.
<https://doi.org/10.2741/2230>
PMID:[17127464](https://pubmed.ncbi.nlm.nih.gov/17127464/)
18. Dobrila-Dintinjana R, Vanis N, Dintinjana M, Radić M. Etiology and oncogenesis of pancreatic carcinoma. *Coll Antropol.* 2012; 36:1063–67.
PMID:[23213974](https://pubmed.ncbi.nlm.nih.gov/23213974/)
19. Zong Z, Song Y, Xue Y, Ruan X, Liu X, Yang C, Zheng J, Cao S, Li Z, Liu Y. Knockdown of LncRNA SCAMP1 suppressed Malignant biological behaviours of glioma cells via modulating miR-499a-5p/LMX1A/NLRCS pathway. *J Cell Mol Med.* 2019; 23:5048–62.
<https://doi.org/10.1111/jcmm.14362>
PMID:[31207033](https://pubmed.ncbi.nlm.nih.gov/31207033/)
20. Zhang J, Castle D. Regulation of fusion pore closure and compound exocytosis in neuroendocrine PC12 cells by SCAMP1. *Traffic.* 2011; 12:600–14.
<https://doi.org/10.1111/j.1600-0854.2011.01170.x>
PMID:[21272170](https://pubmed.ncbi.nlm.nih.gov/21272170/)
21. Diering GH, Church J, Numata M. Secretory carrier membrane protein 2 regulates cell-surface targeting of brain-enriched Na⁺/H⁺ exchanger NHE5. *J Biol Chem.* 2009; 284:13892–903.
<https://doi.org/10.1074/jbc.M807055200>
PMID:[19276089](https://pubmed.ncbi.nlm.nih.gov/19276089/)
22. Liao H, Ellena J, Liu L, Szabo G, Cafiso D, Castle D. Secretory carrier membrane protein SCAMP2 and phosphatidylinositol 4,5-bisphosphate interactions in the regulation of dense core vesicle exocytosis. *Biochemistry.* 2007; 46:10909–20.
<https://doi.org/10.1021/bi701121j>
PMID:[17713930](https://pubmed.ncbi.nlm.nih.gov/17713930/)
23. Liu L, Liao H, Castle A, Zhang J, Casanova J, Szabo G, Castle D. SCAMP2 interacts with Arf6 and phospholipase D1 and links their function to exocytotic fusion pore formation in PC12 cells. *Mol Biol Cell.* 2005; 16:4463–72.
<https://doi.org/10.1091/mbc.e05-03-0231>
PMID:[16030257](https://pubmed.ncbi.nlm.nih.gov/16030257/)
24. Aoh QL, Castle AM, Hubbard CH, Katsumata O, Castle JD. SCAMP3 negatively regulates epidermal growth factor receptor degradation and promotes receptor recycling. *Mol Biol Cell.* 2009; 20:1816–32.
<https://doi.org/10.1091/mbc.e08-09-0894>
PMID:[19158374](https://pubmed.ncbi.nlm.nih.gov/19158374/)

25. Falguières T, Castle D, Gruenberg J. Regulation of the MVB pathway by SCAMP3. *Traffic*. 2012; 13:131–42. <https://doi.org/10.1111/j.1600-0854.2011.01291.x> PMID:[21951651](#)
26. Li J, Belogortseva N, Porter D, Park M. Chmp1A functions as a novel tumor suppressor gene in human embryonic kidney and ductal pancreatic tumor cells. *Cell Cycle*. 2008; 7:2886–93. <https://doi.org/10.4161/cc.7.18.6677> PMID:[18787405](#)
27. Krebs CJ, Pfaff DW. Expression of the SCAMP-4 gene, a new member of the secretory carrier membrane protein family, is repressed by progesterone in brain regions associated with female sexual behavior. *Brain Res Mol Brain Res*. 2001; 88:144–54. [https://doi.org/10.1016/s0169-328x\(01\)00043-2](https://doi.org/10.1016/s0169-328x(01)00043-2) PMID:[11295240](#)
28. Han C, Chen T, Yang M, Li N, Liu H, Cao X. Human SCAMP5, a novel secretory carrier membrane protein, facilitates calcium-triggered cytokine secretion by interaction with SNARE machinery. *J Immunol*. 2009; 182:2986–96. <https://doi.org/10.4049/jimmunol.0802002> PMID:[19234194](#)
29. Hu J, Hu H, Hang JJ, Yang HY, Wang ZY, Wang L, Chen DH, Wang LW. Simultaneous high expression of PLD1 and Sp1 predicts a poor prognosis for pancreatic ductal adenocarcinoma patients. *Oncotarget*. 2016; 7:78557–65. <https://doi.org/10.18632/oncotarget.12447> PMID:[27713167](#)
30. Fitzgerald TL, Lertpiriyapong K, Cocco L, Martelli AM, Libra M, Candido S, Montalto G, Cervello M, Steelman L, Abrams SL, McCubrey JA. Roles of EGFR and KRAS and their downstream signaling pathways in pancreatic cancer and pancreatic cancer stem cells. *Adv Biol Regul*. 2015; 59:65–81. <https://doi.org/10.1016/j.jbior.2015.06.003> PMID:[26257206](#)
31. Gore J, Imasuen-Williams IE, Conteh AM, Craven KE, Cheng M, Korc M. Combined targeting of TGF- β , EGFR and HER2 suppresses lymphangiogenesis and metastasis in a pancreatic cancer model. *Cancer Lett*. 2016; 379:143–53. <https://doi.org/10.1016/j.canlet.2016.05.037> PMID:[27267807](#)
32. Bassagañas S, Allende H, Cobler L, Ortiz MR, Llop E, de Bolós C, Peracaula R. Inflammatory cytokines regulate the expression of glycosyltransferases involved in the biosynthesis of tumor-associated sialylated glycans in pancreatic cancer cell lines. *Cytokine*. 2015; 75:197–206. <https://doi.org/10.1016/j.cyto.2015.04.006> PMID:[25934648](#)
33. Hashimoto S, Furukawa S, Hashimoto A, Tsutaho A, Fukao A, Sakamura Y, Parajuli G, Onodera Y, Otsuka Y, Handa H, Oikawa T, Hata S, Nishikawa Y, et al. ARF6 and AMAP1 are major targets of KRAS and TP53 mutations to promote invasion, PD-L1 dynamics, and immune evasion of pancreatic cancer. *Proc Natl Acad Sci USA*. 2019; 116:17450–59. <https://doi.org/10.1073/pnas.1901765116> PMID:[31399545](#)
34. Bustin SA, Benes V, Garson JA, Hellemans J, Huggett J, Kubista M, Mueller R, Nolan T, Pfaffl MW, Shipley GL, Vandesompele J, Wittwer CT. The MIQE guidelines: minimum information for publication of quantitative real-time PCR experiments. *Clin Chem*. 2009; 55:611–22. <https://doi.org/10.1373/clinchem.2008.112797> PMID:[19246619](#)
35. Tsuboi M, Taniuchi K, Furihata M, Naganuma S, Kimura M, Watanabe R, Shimizu T, Saito M, Dabanaka K, Hanazaki K, Saibara T. Vav3 is linked to poor prognosis of pancreatic cancers and promotes the motility and invasiveness of pancreatic cancer cells. *Pancreatol*. 2016; 16:905–16. <https://doi.org/10.1016/j.pan.2016.07.002> PMID:[27453460](#)
36. Miyazawa Y, Uekita T, Hiraoka N, Fujii S, Kosuge T, Kanai Y, Nojima Y, Sakai R. CUB domain-containing protein 1, a prognostic factor for human pancreatic cancers, promotes cell migration and extracellular matrix degradation. *Cancer Res*. 2010; 70:5136–46. <https://doi.org/10.1158/0008-5472.CAN-10-0220> PMID:[20501830](#)
37. Tang Z, Li C, Kang B, Gao G, Li C, Zhang Z. GEPIA: a web server for cancer and normal gene expression profiling and interactive analyses. *Nucleic Acids Res*. 2017; 45:W98–102. <https://doi.org/10.1093/nar/gkx247> PMID:[28407145](#)
38. Vasaikar SV, Straub P, Wang J, Zhang B. LinkedOmics: analyzing multi-omics data within and across 32 cancer types. *Nucleic Acids Res*. 2018; 46:D956–63. <https://doi.org/10.1093/nar/gkx1090> PMID:[29136207](#)
39. Wang J, Vasaikar S, Shi Z, Greer M, Zhang B. WebGestalt 2017: a more comprehensive, powerful, flexible and interactive gene set enrichment analysis toolkit. *Nucleic Acids Res*. 2017; 45:W130–37. <https://doi.org/10.1093/nar/gkx356> PMID:[28472511](#)
40. Ghandi M, Huang FW, Jané-Valbuena J, Kryukov GV, Lo CC, McDonald ER 3rd, Barretina J, Gelfand ET, Bielski CM, Li H, Hu K, Andreev-Drakhlin AY, Kim J, et al. Next-generation characterization of the cancer cell line encyclopedia. *Nature*. 2019; 569:503–08. <https://doi.org/10.1038/s41586-019-1186-3> PMID:[31068700](#)

41. Li H, Ning S, Ghandi M, Kryukov GV, Gopal S, Deik A, Souza A, Pierce K, Keskula P, Hernandez D, Ann J, Shkzoza D, Apfel V, et al. The landscape of cancer cell line metabolism. *Nat Med*. 2019; 25:850–60. <https://doi.org/10.1038/s41591-019-0404-8> PMID:31068703
42. Cancer Cell Line Encyclopedia Consortium, and Genomics of Drug Sensitivity in Cancer Consortium. Pharmacogenomic agreement between two cancer cell line data sets. *Nature*. 2015; 528:84–87. <https://doi.org/10.1038/nature15736> PMID:26570998
43. Barretina J, Caponigro G, Stransky N, Venkatesan K, Margolin AA, Kim S, Wilson CJ, Lehár J, Kryukov GV, Sonkin D, Reddy A, Liu M, Murray L, et al. The cancer cell line encyclopedia enables predictive modelling of anticancer drug sensitivity. *Nature*. 2012; 483:603–07. <https://doi.org/10.1038/nature11003> PMID:22460905
44. Li W, Cowley A, Uludag M, Gur T, McWilliam H, Squizzato S, Park YM, Buso N, Lopez R. The EMBL-EBI bioinformatics web and programmatic tools framework. *Nucleic Acids Res*. 2015; 43:W580–84. <https://doi.org/10.1093/nar/gkv279> PMID:25845596
45. Papatheodorou I, Fonseca NA, Keays M, Tang YA, Barrera E, Bazant W, Burke M, Füllgrabe A, Fuentes AM, George N, Huerta L, Koskinen S, Mohammed S, et al. Expression atlas: gene and protein expression across multiple studies and organisms. *Nucleic Acids Res*. 2018; 46:D246–51. <https://doi.org/10.1093/nar/gkx1158> PMID:29165655
46. Uhlén M, Fagerberg L, Hallström BM, Lindskog C, Oksvold P, Mardinoglu A, Sivertsson Å, Kampf C, Sjöstedt E, Asplund A, Olsson I, Edlund K, Lundberg E, et al. Proteomics. Tissue-based map of the human proteome. *Science*. 2015; 347:1260419. <https://doi.org/10.1126/science.1260419> PMID:25613900
47. Thul PJ, Åkesson L, Wiking M, Mahdessian D, Geladaki A, Ait Blal H, Alm T, Asplund A, Björk L, Breckels LM, Bäckström A, Danielsson F, Fagerberg L, et al. A subcellular map of the human proteome. *Science*. 2017; 356:eaal3321. <https://doi.org/10.1126/science.aal3321> PMID:28495876
48. Uhlen M, Zhang C, Lee S, Sjöstedt E, Fagerberg L, Bidkhori G, Benfeitas R, Arif M, Liu Z, Edfors F, Sanli K, von Feilitzen K, Oksvold P, et al. A pathology atlas of the human cancer transcriptome. *Science*. 2017; 357:eaan2507. <https://doi.org/10.1126/science.aan2507> PMID:28818916
49. Cerami E, Gao J, Dogrusoz U, Gross BE, Sumer SO, Aksoy BA, Jacobsen A, Byrne CJ, Heuer ML, Larsson E, Antipin Y, Reva B, Goldberg AP, et al. The cBio cancer genomics portal: an open platform for exploring multidimensional cancer genomics data. *Cancer Discov*. 2012; 2:401–04. <https://doi.org/10.1158/2159-8290.CD-12-0095> PMID:22588877
50. Gao J, Aksoy BA, Dogrusoz U, Dresdner G, Gross B, Sumer SO, Sun Y, Jacobsen A, Sinha R, Larsson E, Cerami E, Sander C, Schultz N. Integrative analysis of complex cancer genomics and clinical profiles using the cBioPortal. *Sci Signal*. 2013; 6:p11. <https://doi.org/10.1126/scisignal.2004088> PMID:23550210
51. Szklarczyk D, Gable AL, Lyon D, Junge A, Wyder S, Huerta-Cepas J, Simonovic M, Doncheva NT, Morris JH, Bork P, Jensen LJ, Mering CV. STRING v11: protein-protein association networks with increased coverage, supporting functional discovery in genome-wide experimental datasets. *Nucleic Acids Res*. 2019; 47:D607–13. <https://doi.org/10.1093/nar/gky1131> PMID:30476243
52. Warde-Farley D, Donaldson SL, Comes O, Zuberi K, Badrawi R, Chao P, Franz M, Grouios C, Kazi F, Lopes CT, Maitland A, Mostafavi S, Montojo J, et al. The GeneMANIA prediction server: biological network integration for gene prioritization and predicting gene function. *Nucleic Acids Res*. 2010; 38:W214–20. <https://doi.org/10.1093/nar/gkq537> PMID:20576703

SUPPLEMENTARY MATERIALS

Supplementary Figure



Supplementary Figure 1. The difference in SCAMP1 and SCAMP5 between early stage and late stages as diagnosis markers. (A, B) The significant difference in SCAMP1 ($p < 0.05$) and SCAMP5 ($p < 0.05$) between early stage (Stage I + II) and late stages (Stage III + IV) as diagnosis markers. (C, D) The difference in SCAMP1 ($p > 0.05$) (C) and SCAMP5 ($p < 0.05$) (D) between early stages (Stage I + II a) and late stages (Stage II b + III + IV). The Area Under the Curve (AUC) metrics are also provided for SCAMP1 and 5 to predict diagnosis in PAAD by Medcalc.

Supplementary Table

Supplementary Table 1. The most significant genes-Top 10 correlated with SCAMPs 1 and 5 by cBioPortal.

SCAMP1			SCAMP5				
	Correlated gene	Spearman's correlation	p-Value		Correlated gene	Spearman's correlation	p-Value
POSITIVE	TMED7	0.741659	1.62E-32	POSITIVE	BEX1	0.785973	8.28E-39
	COL4A3BP	0.736721	6.78E-32		OGDHL	0.775737	3.15E-37
	PJA2	0.717279	1.41E-29		RUNDC3A	0.755899	2.16E-34
	PPM1A	0.717126	1.46E-29		CHGA	0.751231	9.19E-34
	TNPO1	0.716946	1.53E-29		AMER3	0.749632	1.50E-33
	UBL3	0.710301	8.57E-29		TMEM63C	0.744419	7.18E-33
	TMEM167A	0.698749	1.52E-27		KCNJ11	0.743529	9.34E-33
	C5ORF24	0.687555	2.17E-26		ABCC8	0.741569	1.66E-32
	BDP1	0.684726	4.18E-26		SCGN	0.741037	1.94E-32
	AKAP11	0.682395	7.12E-26		DUSP26	0.740452	2.31E-32
NEGATIVE	DAZAP1	-0.67272	6.16E-25	NEGATIVE	TGIF1	-0.57208	6.01E-17
	CYBC1	-0.65368	3.43E-23		NDE1	-0.54588	2.73E-15
	PFN1	-0.64466	2.09E-22		HRH1	-0.53127	1.99E-14
	BCL2L12	-0.634	1.63E-21		MET	-0.52996	2.37E-14
	GALK1	-0.6296	3.73E-21		FAM83D	-0.50956	3.23E-13
	IKBKG	-0.62792	5.09E-21		ECT2	-0.50923	3.36E-13
	RHOG	-0.62117	1.75E-20		TEAD3	-0.50606	4.96E-13
	RPS6KB2	-0.61867	2.74E-20		CDC25C	-0.50488	5.73E-13
	ALDH16A1	-0.61025	1.21E-19		TFAP2A	-0.49735	1.42E-12
	RPLP1	-0.60608	2.48E-19		TRIM59	-0.49657	1.56E-12

The most significant genes-Top 10 correlated with SCAMPs 1 and 5 by cBioPortal.